JOURNAL OF BACTERIOLOGY, May 1985, p. 598–606
0021-9193/85/050598-09$02.00/0

Vol. 162, No. 2

Physical Analysis of Deletion Mutations in the *ilvGEDA* Operon of *Escherichia coli* K-12

RICHARD P. DRIVER AND ROBERT P. LAWTHER*

Department of Biology, University of South Carolina, Columbia, South Carolina 29208

Received 21 September 1984/Accepted 4 February 1985

DNA-DNA hybridization of cloned segments of the *Escherichia coli* K-12 *ilvGEDA* operon to genomic blots was used to determine the physical dimensions of a series of deletion mutations of the *ilvGEDA* operon. The smallest mutation resulted from the deletion of approximately 200 base pairs from within *ilvD*, whereas the largest mutation resulted from the deletion of 17 kilobases including the *rep* gene. The structure of three of these mutants indicates that formation of the deletions was mediated by Tn*5* (or Tn*5*-131) that is retained in the chromosome. This is the first observation of this type of Tn*5*-mediated event. Our analysis of the total acetohydroxy acid synthase activity of strains containing deletions of *ilvG* indicates that the truncated *ilvG* polypeptide of wild-type *E. coli* K-12 lacks enzyme activity. The small 200-base-pair deletion of *ilvD* confirms the presence of a strong polar site 5′ to *ilvA*. The detailed structure of these deletions should prove useful for the investigation of other genes in this region. This genomic analysis demonstrates that the *ilv* restriction site map that was established previously by the analysis of recombinant bacteriophage and plasmids is identical to that on the genome.

The structural genes for the biosynthesis of isoleucine and valine are divided into several transcriptional units located at three sites in the *Escherichia coli* K-12 genome (1). The largest of these is the *ilvGEDA* operon, which along with *ilvY* and *ilvC*, is located at 84 min on the *E. coli* K-12 map. Several deletion mutations of this operon have been isolated and partially characterized; the first isolated of these was the Δ(*ilvDAYC-rep*)*115* mutant. It was isolated by UV mutagenesis and initially reported to be a deletion of *ilvD* and *ilvC* (17). However, subsequent biochemical analysis indicated that this deletion included *ilvA* (18, 23). A second deletion, Δ(*ilvGEDAYC-rep*)*2049*, was reported by Watson et al. (39). A λ bacteriophage secondary attachment site is present in *ilvC* (41), and the bacteriophage λy199 (40) was integrated into this site. The Δ(*ilvGEDAYC-rep*)*2049* deletion was isolated in a strain that survived the thermal induction of the bacteriophage from the *ilvC* att site (39). The spontaneous Δ*ilvD2076* mutant was reported to be an *ilvDA* deletion (33). More recently a set of deletions have been isolated by a novel method using the *ilvA700*::Tn*5* mutation and the bacteriophage λ *b*221 *c*I857 *rex*::Tn*5*-131 (3). The bacteriophage was integrated into the *E. coli* K-12 chromosome by homologous recombination between IS*50* elements of Tn*5* and Tn*5*-131. The deletions were isolated as survivors of the thermal induction of the bacteriophage. This selection yielded a set of mutant strains that contained deletions of various lengths of the operon, and each mutant retained either Tn*5* or Tn*5*-131.

Deletion mutations have proved to be useful tools in the analysis of gene structure and expression. In part, their utility depends upon genetically defining the extent of each deletion. Although they have been used in studies of the operon, the extent of the *ilvGEDA* deletions has not been ascertained. For example, the (*ilvDAYC-rep*)*115* and (*ilvGEDAYC-rep*)*2049* deletions were used to study *ilvC* expression (39), and more recently the deletions generated from *ilvA700*::Tn*5* were used to investigate *ilvG* expression (3). To extend the analysis of the expression of the *ilvGEDA* operon, it is essential to establish the structures and define the limits of these deletions. The restriction site map of these genes offered a ready means for their analysis by the use of DNA-DNA hybridization of genomic digests with cloned portions of the *ilvGEDA* operon.

MATERIALS AND METHODS

Bacterial strains, plasmids, and media. The relevant genotypes of the *E. coli* K-12 strains used in this work are listed in Table 1. The plasmids used are listed in Table 2, and their physical relationships relative to the *ilvGEDA* genes or Tn*5* are diagrammed in Fig. 1. Luria broth (LB) and M63 minimal media were prepared as described by Miller (26). Vogel-Bonner minimal E (VBE) medium was prepared as described by Davis et al. (6). Media were supplemented with antibiotics and amino acids as required.

Enzymes. Restriction endonucleases and T4 DNA ligase were obtained from New England Biolabs. *E. coli* DNA polymerase I was obtained from Boehringer Mannheim Biochemicals. DNase I was obtained from Worthington Diagnostics, lysozyme was from Sigma Chemical Co., and proteinase K was from E. M. Biochemicals.

Materials. All antibiotics, amino acids, and other medium supplements were obtained from Sigma. Agarose was obtained from Bio-Rad Laboratories. Cesium chloride was obtained from Kawecki Berylco Industries, Reading, Pa. Nucleotide triphosphates were obtained from P. L. Biochemicals, and [α^{32}-P]dATP was obtained from New England Nuclear Corp.

DNA isolation. *E. coli* K-12 genomic DNA was prepared as follows. A 20-ml LB culture was grown to a cell density of 6 × 10^8 cells per ml (equal to 200 Klett units, monitored with a Klett-Summerson colorimeter with a no. 54 green filter). The culture was chilled to 4°C and was harvested by centrifugation at 5,000 rpm (3,000 × *g*) for 5 min in a

* Corresponding author.

TABLE 1. *E. coli* K-12 strains

Strain	Relevant genotype or phenotype	Source (Reference)
CBK317	Δ*ilvDA722*::Tn*5 recA*	
CBK708	Δ *ilvGEDA724*::Tn*5*-131 Δ(*pro-lac*) *thyA*	C. Berg (3)
CBK718	Δ*ilvGEDAY723*::Tn*5* Δ(*pro-lac*) *thyA*	C. Berg (3)
CU452	Δ(*ilvDAYC-rep*)*115 trp arg* Δ*lac*	D. Calhoun (33)
CU505	Δ(*ilvGEDAYC-rep*)*2049 leu-455 galT12*	D. Calhoun (38)
CU655	Δ*ilvD2076 leu-455 galT12 rbs-221*	D. Calhoun (32)
FD1004	*rbs-301*::Tn*10 ilvG468*(IlvG$^+$) *trpEam9829 trpAam9829*	This laboratory
FD1005	*rbs-302*::Tn*5 ilvG468*(IlvG$^+$) *trpEam9829 trpAam9829*	This laboratory
FD1011	*rbs-302*::Tn*5* Δ*ilvGEDA724*::Tn*5*-131 Δ(*pro-lac*) *thyA*	CBK708 × FD1005
FD1015	*rbs-301*::Tn*10* Δ*ilvGEDA723*::Tn*5* Δ(*pro-lac*) *thyA*	CBK718 × FD1004
FD1037	*rbs-302*::Tn*5* Δ(*ilvGEDAYC-rep*)*2049 leu-455 galT12*	CU505 × FD1004
FD1038	*rbs-302*::Tn*5* Δ(*ilvDAYC-rep*)*115 trp arg* Δ*lac*	CU452 × FD1004
FD1040	*rbs-302*::Tn*5* Δ(*ilvDAYC-rep*)*115 galK galU* Δ*lacX74*	M182 × FD1038
FD1042	*rbs-302*::Tn*5* Δ(*ilvGEDAYC-rep*)*2049 galK galU* Δ*lacX74*	M182 × FD1037
FD1049	*rbs*-301::Tn10 Δ*ilvGEDA723*::Tn*5* Δ(*ara-leu-ilvIH*)*863 ilvB800*::Mu 1 *thi-1 trpR*	PS1283 × FD1015
FD1050	*rbs-302*::Tn*5* Δ*ilvGEDA724*::Tn*5*-131 Δ(*ara-leu-ilvIH*)*863 ilvB800*::Mu 1 *thi-1 trpR*	PS1283 × FD1011
FD1055	*rbs-301*::Tn*10* Δ*ilvGEDA723*::Tn*5 trpEam9829 trpAam9761 thi-1*	T31-4-4 × FD1015
FD1056	*rbs-302*::Tn*5* Δ(*ilvGEDA724*::Tn*5*-131 *trpEam9829 trpAam9761 thi-1*	T31-4-4 × FD1011
FD1069	*rbs-302*::Tn*5* Δ(*ilvGEDAYC-rep*)*2049 trpEam9827 trpAam9761 thi-1*	T31-4-4 × FD1037
M182	*galK galU* Δ*lacX74*	M. Casdaban
PS1283	Δ(*ara-leu-ilvIH*)*863 ilvB800*::Mu 1 *rbs-115 thi-1 trpR*	J. Calvo (28)
Q359	P2 lysogen	J. Kuhn
T31-4-4	*trpEam9829 trpAam9761 thi-1*	This laboratory (20)

Beckman JA20 rotor. The cell pellet was washed twice with 10 ml of cold VBE, and the cells were collected by centrifugation as described above. The cell pellet was suspended in 2.0 ml of 50 mM Tris-hydrochloride (pH 8.0)–50 mM EDTA–15% sucrose containing 2 mg of freshly added lysozyme per ml and incubated at 4°C for 15 min. The cells were lysed by the addition of 0.05 ml 10% sodium dodecyl sulfate and digested with proteinase K (0.1 mg/ml) for 2 h at 65°C. After the addition of 2.0 ml of water, the lysate was extracted with equal volumes of water-saturated phenol (2×), 1:1 mixture of phenol-chloroform (1×), and chloroform (1×). The samples were digested for 2 h at 37°C with RNase A (0.1 mg/ml) and extracted with an equal volume of phenol-chloroform. The resulting DNA solution was dialyzed for 8 to 12 h two times each against 1 liter of 25 mM EDTA (pH 8.0) and TE buffer (10 mM Tris-hydrochloride, 1 mM EDTA, pH 8.0).

Plasmid DNA was prepared by a modification of the technique of Davis et al. (7). A 250-ml LB culture in a 2-liter baffled flask was grown to 170 Klett units. After the addition of 50 mg of chloramphenicol, the culture was incubated an additional 12 to 15 h and harvested by centrifugation for 10 min at 5,000 rpm (4,400 × *g*) in a Beckman JA10 rotor. The cells were suspended in 25 ml of 100 mM NaCl–10 mM EDTA–50 mM Tris-hydrochloride (pH 8.0), transferred to 50-ml polycarbonate tubes, and collected by centrifugation for 10 min at 5,000 rpm (3,000 × *g*) in a Beckman JA20 rotor. The cell pellet was suspended in 10 ml of 15% sucrose–50 mM EDTA–50 mM Tris-hydrochloride (pH 8.0) containing 2 mg of lysozyme per ml. After a 10-min incubation at room temperature, 0.5 ml of 10% sodium dodecyl sulfate was added, and the cells were lysed by gentle mixing. One milliliter of 5 M potassium acetate was added, and cell lysate was gently mixed. After a 30-min incubation on ice, the lysate was clarified by centrifugation at 20,000 rpm (48,400 × *g*) for 30 min in a Beckman JA20 rotor at 4°C. The supernatant was collected, and 0.05 ml of RNase A (2 mg/ml) was added. After 30 min at room temperature, the lysate was extracted with 10 ml of water-saturated phenol. The upper phenolic phase was discarded, and the aqueous phase was extracted with 10 ml of chloroform. Nucleic acids were precipitated with ethanol, suspended in 5.0 ml 0.3 M sodium acetate, and reprecipitated. The nucleic acid pellet was suspended in 2.5 ml of 50 mM NaCl–5 mM EDTA–50 mM Tris-hydrochloride (pH 8.0), and 2.6 g of CsCl was added. After the addition of 0.150 ml of ethidium bromide (10 mg/ml), the refractive index was adjusted to 1.390. Plasmid DNA was prepared by centrifugation at 80,000 rpm (510,000 × *g*) for 4 h at 20°C in a Beckman VTi80 rotor. The plasmid band was collected by side puncture, and ethidium bromide was extracted with CsCl-saturated isopropanol. The DNA was diluted with 4 volumes of TE and precipitated with ethanol. The DNA was suspended in 2.0 ml of TE; after the addition of 1.0 ml of 7.5 M ammonium acetate, the DNA was precipitated with ethanol. This process was repeated, and the DNA was precipitated a final time from 0.3 M sodium acetate. The DNA pellet was suspended in 0.3 ml of TE.

TABLE 2. Plasmids used as hybridization probes

Plasmid	Restriction fragment	Genotype	Source
pJG31	7.4-kb *Hin*dIII insert into pBR322	*rho*	D. Calhoun
pLC26-3	8.0-kb insert into col E1	*ilvGEDA*	G. W. Hatfield
pRL5	4.8-kb *Hin*dIII insert into pBR322	*ilvGE'*	This laboratory
pRD125	1.7-kb *Hin*dIII insert into pBR322	*ilv'ED'*	This laboratory
pRD129	1.4-kb *Hin*dIII-*Sal*I insert into pBR322	*ilv'DA'*	This laboratory
pRD130	0.8-kb *Sal*I-*Eco*RI insert into pBR322	*ilvA'*	This laboratory
pRD131	0.8-kb PvuII-*Sal*I insert into pBR322	*ilvG'*	This laboratory
pRD150	8.0-kb *Hin*dIII insert into pBR322	*ilv'DAYC*	This laboratory
pRD151	1.0-kb *Xho*I-*Bgl*II insert into pBR322	IS*50'*	This laboratory

Genetic techniques. P1 bacteriophage-mediated transduction was accomplished by standard techniques. Restriction

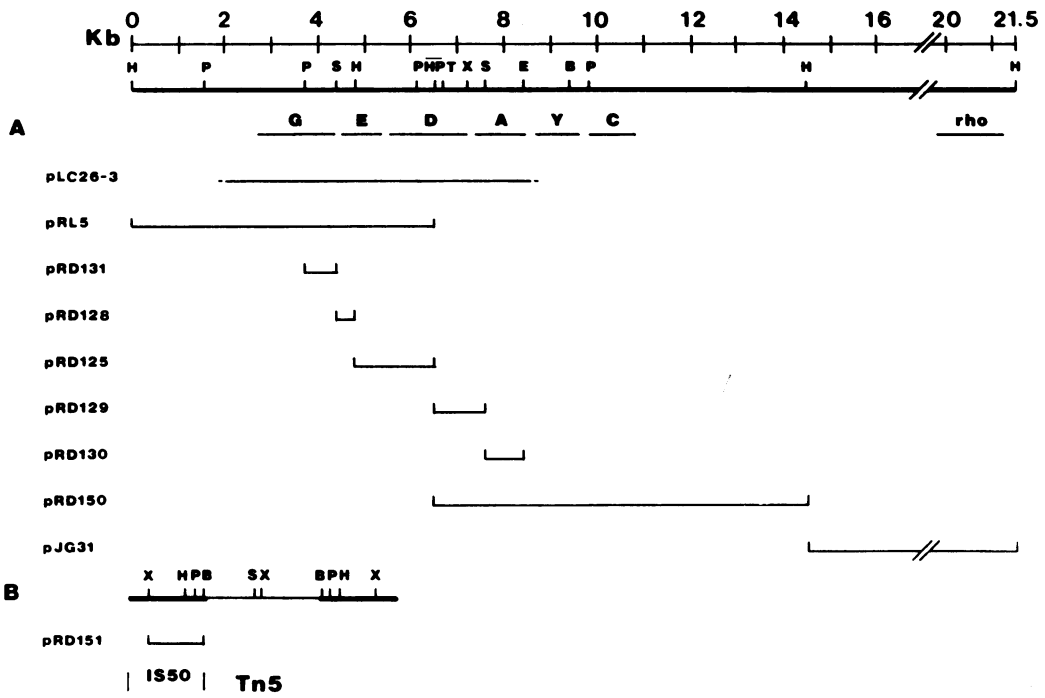

FIG. 1. Diagram of the physical relationship of the *ilvGEDA* probes to the operon (A) and pRD151 to Tn*5* (B). The restriction map of Tn*5* is based upon references 2 and 16. Restriction endonuclease cleavage sites are indicated by the following letters: B, *Bgl*II; E, *Eco*RI; H, *Hin*dIII; P, *Pvu*II; S, *Sal*I; T, *Pst*I; X, *Xho*I.

endonuclease digestions were performed as suggested by New England Biolabs, and restriction fragments were isolated as described by Maxam and Gilbert (24). Insertion of restriction fragments into plasmid vectors and subsequent analyses were by standard recombinant DNA techniques (6, 22).

Southern hybridizations. Approximately 2 μg of DNA from each *E. coli* K-12 strain was digested with the appropriate restriction endonuclease(s). The products of digestion were separated by electrophoresis on an 0.8% agarose gel containing 100 mM Tris-acetate (pH 8.05), 40 mM sodium acetate, and 4 mM EDTA. After electrophoresis, the DNA restriction fragments were transferred to nitrocellulose (35). DNA probes were labeled by nick translation as described by Davis et al. (6), except that labeled DNA was separated from unicorporated nucleotides by precipitation with spermine (14). Filters were prehybridized at 42°C for 1 h in 0.9 M NaCl, 50 mM NaH_2PO_4 [pH 7.4], 5 mM EDTA, 5× Denhardt solution (0.1% [wt/vol] each of bovine serum albumin, Ficoll 400,000, and polyvinylpyrrolidine), 0.3% sodium dodecyl sulfate, 100 μg of sonically disrupted, denatured calf thymus DNA per ml, and 50% formamide. After 1 h, 10^6 to 10^8 cpm of denatured, ^{32}P-labeled probe was added. After 24 h, the filters were washed as described by Davis et al. (6). An *Hin*dIII restriction endonuclease digestion of the bacteriophage lambda was included on each agarose gel, and DNA extracted from strain T31-4-4 served as a wild-type control. The size of hybrid restriction fragments was determined by direct comparison of the autoradiogram and a photograph of the ethidium bromide-stained agarose gel.

RESULTS

Analysis of deletions generated from *ilvA700*::Tn*5*. The *ilvGEDA724*::Tn*5*-131, *ilvGEDA723*::Tn*5*, and *ilvDA722*::Tn*5* mutations were all generated in a strain that was lysogenized with λ *b*221 *c*I857 *rex*::Tn*5*-131 by homologous recombination with *ilvA700*::Tn*5*. The mutations were selected as survivors of the thermal induction of the bacteriophage, and the extent of each deletion was characterized by assaying for the enzyme products of the operon (3). To ascertain more precisely the structure of each deletion, chromosomal DNA was isolated and digested with a series of restriction endonucleases, and *ilv*-specific fragments were identified by DNA blot hybridization.

The probe for the intact *ilvGEDA* operon (pLC26-3) hybridized with three *Pvu*II restriction fragments from wild-type DNA (Table 3). The 1.8-kilobase (kb) fragment includes the promotor-attenuator and the proximal portion of *ilvG* (from 1.9 to 3.7 kb in Fig. 1 and 2). The 2.5-kb fragment includes the distal portion of *ilvG* through the beginning of *ilvD* (from 3.7 to 6.2 kb), and the largest fragment extends from *ilvD* to within *ilvC* (6.3 to 9.8 kb). The small 0.2-kb fragment from within *ilvD* was not observed in these experiments.

The largest *Pvu*II restriction fragment from each of the deletions was smaller than that from wild-type DNA (Table 3). This is the result of the original insertion of Tn*5* into *ilvA*. The IS*50* terminal repeat of Tn*5* contains a *Pvu*II site (Fig. 1), and the 3.3-kb *Pvu*II fragment extends from the IS*50* terminus closest to *ilvC* to the *Pvu* II restriction site within *ilvC*. The identical size of this fragment from each deletion reflects their common ancestry and indicates that the original Tn*5* insertion occurred approximately 1.8 to 2.0 kb from the *Pvu*II site in *ilvC*. The 2.5- and 1.8-kb *Pvu*II restriction fragments are present in DNA from CBK317 (Δ*ilvDA722*::Tn*5*), indicating that this deletion ends before the *Pvu*II restriction site at 6.2 kb in Fig. 2. The 1.8-kb fragment corresponding to the proximal portion of *ilvG* is present in the DNA from CBK708 (Δ*ilvGEDA723*::Tn*5*). None of the proximal portion of the operon (*ilvGED*) is

TABLE 3. Hybridization analysis of deletions generated from *ilvA700*::Tn*5*

Chromosomal DNA digested with:	Plasmid *ilv* DNA probe	Fragment size (kb) of chromosomal DNA from the indicated *E. coli* strains that hybridized with the indicated probe			
		T31-4-4 (wild type)	CBK317 (Δ*ilvDA722*::Tn*5*)	CBK708 (Δ*ilvGEDA723*::Tn*5*)	CBK718 (Δ*ilvGEDA724*::TN*5*-131)
*Pvu*II	pLC26-3 (*ilvGEDA*)	3.6	3.3	3.3	3.3
		2.5	2.5		
		1.8	1.8	1.8	
*Hin*dIII	pRD125 (*ilv'ED'*)	1.7	2.6		
	pRD129 (*ilv'DA'*)	8.0			
*Sal*I-*Bgl*II	pRD130 (*ilvA'*)	1.9	3.1	3.1	3.1
	pRD151 (IS*50*)		4.5[a]	5.5	
			3.7[a]		
			3.3		3.1
			3.1	3.1	1.6

[a] These bands are due to an unlinked Tn*5*.

present in CBK718 (Δ*ilvGEDA724*::Tn*5*-131) as evidenced by the observation that the hybridization of pLC26-3 is restricted to only the distal 3.3-kb *Pvu*II fragment (Table 3). Since our data indicate that both terminal IS*50* elements are retained (see below), any other *ilv-Pvu*II restriction fragments would be greater than 1.5 kb (the distance separating the *Pvu*II site in IS*50* from the terminus of the element). Thus the *ilvDA722*::Tn*5* and *ilvGEDA723*::Tn*5* deletions must end near the indicated *Pvu*II sites. The DNA from CBK317 (containing the *ilvDA724*::Tn*5* deletion) was further analyzed for the presence of the *Hin*dIII restriction site at 6.4 kb. This was accomplished by hybridization of an *Hin*dIII restriction digest of chromosomal DNA with the adjacent *ilv'ED'* and *ilv'DA'* probes. The *ilv'DA'* probe does not hybridize to the DNA of the *ilvDA722*::Tn*5* mutant strain (Table 3), whereas the *ilv'ED'* probe hybridizes to a 2.6-kb restriction fragment instead of the 1.7-kb wild-type fragment. The size of this *Hin*dIII restriction fragment (2.6 kb) and the known restriction maps of the *ilvGEDA* operon and Tn*5* (Fig. 1) indicate that the *ilvDA722*::Tn*5* mutation ends less than 100 base pairs (bp) distal to the *Pvu*II restriction site in *ilvD* at 6.1 kb.

To characterize further these mutations, it was necessary to establish their structure adjacent to the transposon. Hybridization of an *ilvA'* probe (pRD130) with an *Sal*I-*Bgl*II restriction digest of each mutant strain identified a common 3.1-kb restriction fragment. Since this fragment is larger than the 1.9-kb fragment from wild-type DNA, the Tn*5* transposon must have inserted distal to the *Sal*I restriction site in *ilvA* (at 7.5 kb in Fig. 2). In fact, a fragment of identical size also hydridizes to the IS*50'* probe (pRD151). This fragment must result from digestion at the *Bgl*II restriction site in the distal IS*50* element (relative to the *ilvGEDA* operon) and the *Bgl*II site in *ilvY* (Fig. 2). Hybridization of an *Sal*I-*Bgl*II digest of DNA from CBK317 with the IS*50'* probe identifies four, rather than the expected two, restriction fragments. Two of these, the 4.5- and 3.7-kb restriction fragments, originate from a second Tn*5* that is not associated with the *ilv* operon. The presence of the second Tn*5* element is indicated by the hybridization of a Tn*5* probe to two *Eco*RI restriction fragments present in a digest of the DNA from CBK317, only one of which hybridizes to pLC26-3 (unpublished observation). The fourth band of 3.3 kb must be the product of digestion at the *Sal*I site in *ilv* at 4.3 kb (Fig. 2) and the *Bgl*II site in the proximal IS*50* element (relative to the *ilvGEDA* operon). Again the size of this fragment indicates that *ilvDA722*::Tn*5* mutation deletes DNA immediately distal to the *Pvu*II site at 6.1 kb in Fig. 1. Hybridization of an *Sal*I-*Bgl*II digest of DNA from CBK708 with pRD151 identifies the 3.1-kb fragment and a 5.4-kb fragment that would

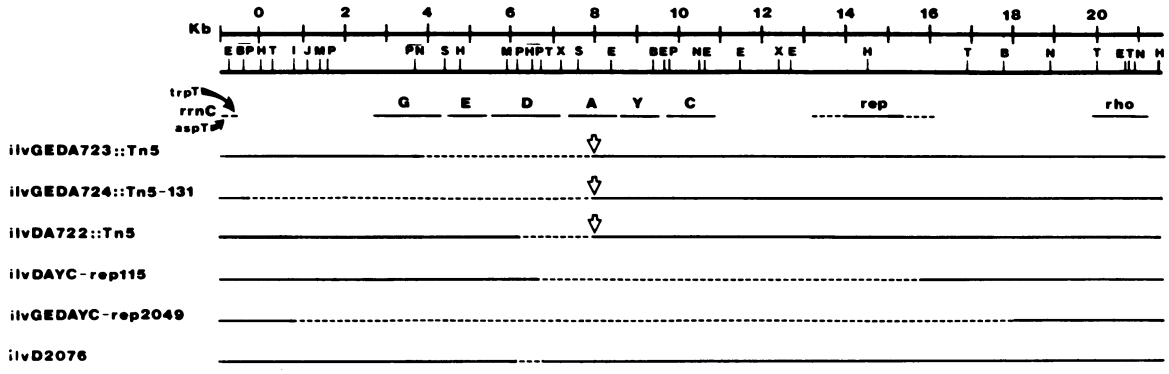

FIG. 2. Restriction site map of the *ilv* region of *E. coli* K-12 and physical map of deletions Δ*ilvGEDA723*::Tn*5*, Δ*ilvGEDA724*::Tn*5*-131, Δ*ilvDA722*::Tn*5*, Δ(*ilvDAYC-rep*)*115*, Δ(*ilvGEDAYC-rep*)*2049*, and Δ*ilvD2076*. The dotted lines represent deleted sequences. Open arrows indicate the site of insertion of Tn*5* or Tn*5*-131. Restriction endonuclease cleavage sites are indicated by the following letters: B, *Bgl*II; E, *Eco*RI; H, *Hin*dIII; I, *Hinc*II; J, *Hpa*I; N, *Kpn*I; T, *Pst*I; P, *Pvu*II; M, *Sma*I; S, *Sal*I; X, *Xho*I. The restriction map is based on published (4, 11, 15, 27, 37) and unpublished data.

extend from the *Bgl*II site at −0.3 kb (Fig. 2) to the *Bgl*II site in the proximal IS*50* element. Hybridization of pRD151 with an *Sal*I-*Bgl*II digest of DNA from CBK718 identifies the common 3.1-kb fragment and a 1.6-kb restriction fragment. This fragment results from digestion at the *Bgl*II site at −0.3 kb (Fig. 1) and the *Bgl*II site in the proximal IS*50* element. This deletion must end before the *Bgl*II site at −0.3 kb because continuation beyond this *Bgl*II site would result in the lethal deletion of the single tryptophanyl-tRNA gene, *trpT* (13, 42). Thus, the *ilvDA722*::Tn*5* mutation deletes approximately 1.8 kb, the *ilvGEDA723*::Tn*5* mutation deletes approximately 4 kb, and the *ilvGEDA724*::Tn*5*-131 mutation deletes approximately 8 kb.

Based upon a comparison of the level of the activity of acetohydroxy acid synthase (AHAS) in this series of *ilvGEDA* operon deletions, Berg et al. (3) concluded that the truncated AHAS II polypeptide from the *ilvG* wild-type gene retained some enzymatic activity. In particular, they found that the total AHAS activity in a strain containing the *ilvGEDA724*::Tn*5*-131 deletion was one-third that of a strain with the *ilvGEDA723*::Tn*5* deletion. Our analysis of *ilvGEDA723*::Tn*5* mutant indicates that it does not disrupt the DNA sequence that encodes the wild-type truncated *ilvG* protein (18), whereas the *ilvGEDA724*::Tn*5*-131 mutation deletes all of *ilvG*. In contrast to their results, our analysis of total AHAS activity indicates that the truncated wild-type protein lacks enzymatic activity. To insure that alterations in AHAS activities resulted solely from these mutations, they were transduced into our wild-type *E. coli* strain (T31-4-4) and assayed for AHAS activity (Table 4). The presence of these two deletions does not dramatically effect total AHAS activity in these strains. Introducing the *ilvGEDA723*::Tn*5* mutant results in a 28% increase in AHAS activity, whereas introducing *ilvGEDA724*::Tn*5*-131 results in a 24% decrease. Introduction of the (*ilvGEDAYC-rep*)2049 deletion (which also deletes all of *ilvG*) yielded a similar decrease in AHAS activity. As a further check, the *ilvGEDA723*::Tn*5* and *ilvGEDA724*::Tn*5*-131 mutations were transduced into strain PS1283 (27), which lacks functional AHAS I (*ilvB*) and AHAS III (*ilvIH*). The level of AHAS activity in strain PS1283 is almost 40-fold lower than that in strain T31-4-4. This low level of activity is unaffected by the presence of the two *ilvGEDA* deletions, further indicating that the truncated wild-type *ilvG* polypeptide does not have AHAS activity.

Analysis of the (*ilvDAYC-rep*)*115* and (*ilvGEDAYC-rep*)*2049* deletions. Hybridization of *Hin*dIII-digested DNA from CU452 with a series of *ilv* probes (Table 5) indicated that the (*ilvDAYC-rep*)*115* deletion starts distal to the *Hin*dIII restriction site at 6.4 kb (Fig. 1 and 2). *Hin*dIII fragments of DNA from CU452 of identical size to those in wild-type DNA hybridized with both pRL5 and pRD125, whereas DNA from CU452 did not hybridize with either pRD129 or pRD150. Digestion of DNA from CU452 with *Pst*I and subsequent hybridization with pRD125 indicates that the *Pst*I restriction site at 6.6 kb (Fig. 1 and 2) is deleted from this allele. The distal terminus of the (*ilvDAYC-rep*)*115* deletion was determined by comparison of the hybridization of the *rho* probe (pJG31) with wild-type DNA and DNA from CU452 (Table 5). *Hin*dIII and *Pst*I digests indicate that the (*ilvDAYC-rep*)*115* deletion ends between the *Hin*dIII site at 14.5 kb and the *Pst*I site at 16.9 kb (Fig. 2). From these digests and other data not presented here, we concluded that the (*ilvDAYC-rep*)*115* mutation deletes DNA from approximately 6.6 to 15.9 kb in Fig. 2.

DNA from CU505, Δ(*ilvGEDAYC-rep*)*2049*, does not hybridize with either the plasmid pLC26-3 or pRD150 (Fig. 1), indicating that this mutation deletes all of the *ilv* genes. However, an *Hin*dIII digest of the DNA from CU505 does hybridize with pRL5 and pJG31 (Fig. 1, Table 5), indicating that CU505 retains DNA sequences before 2 kb and DNA beyond 20 kb (Fig. 1 and 2). Comparison of the hybridization of pRL5 with both *Sal*I-*Hpa*I and *Hin*cII digests of DNA from CU505 (Table 5) with similar digests of DNA from wild-type *E. coli* K-12 indicate that one end of the (*ilvGEDAYC-rep*)*2049* deletion lies between the *Hin*cII site at 0.8 kb and the *Hpa*I site at 1.1 kb. To determine the position of the other terminus of this deletion, DNA from the wild type and from CU505 was digested with a series of

TABLE 4. Effects of deletions of the *ilvGEDA* operon on AHAS activity[a]

Strain	Relevant genotype	AHAS sp act[b]
T31-4-4	Wild type (IlvG⁻)	17.7
FD1055	Δ*ilvGEDA723*::Tn*5*	22.6
FD1056	Δ*ilvGEDA724*::Tn*5*-131	13.4
FD1069	Δ(*ilvGEDAYC-rep*)*2049*	13.7
PS1283	Δ(*ara-leu-ilvIH*)*863* *ilvB800*::Mu 1	0.5
FD1049	Δ*ilvGEDA723*::Tn*5* Δ(*ara-leu-ilvIH*)*863* *ilvB800*::Mu 1	0.5
FD1050	Δ*ilvGEDA724*::Tn*5*-131 Δ(*ara-leu-ilvIH*)*863* *ilvB800*::Mu 1	0.3

[a] Cultures were grown in M63 minimal medium containing 0.25 mM tryptophan, 0.5 mM isoleucine, 0.5 mM leucine, 1.0 mM valine, and 2 μg of thiamine hydrochloride per ml.

[b] Assayed as described by Berg et al. (3). Specific activity in nanomoles per minute per milligram of protein.

TABLE 5. Hybridization analysis of Δ(*ilvDAYC-rep*)*115* and Δ(*ilvGEDAYC-rep*)*2049*

Chromosomal DNA digested with:	Plasmid *ilv* DNA probe	Fragment size (kb) of chromosomal DNA from the indicated *E. coli* strains that hybridized with the indicated probe		
		T31-4-4 (wild type)	CU452 [Δ(*ilvDAYC-rep*)*115*]	CU505 [Δ(*ilvGEDAYC-rep*)*2049*]
*Hin*dIII	pRL5 (*ilvGE'*)	4.8	4.8	4.3
	pRD125 (*ilv'ED'*)	1.7	1.7	
	pRD129 (*ilv'DA'*)	8.0		
	pRD150 (*ilv'DAYC*)	8.0		
*Pst*I	pRD125	6.7	7.7	
*Sal*I-*Hpa*I	pRL5 (*ilvGE'*)	3.5 2.5		
*Hin*cII	pRL5 (*ilvGE'*)	3.8 2.2		3.8
*Hin*dIII	pJG31 (*rho*)	7.4	5.7	4.4
*Pst*I	pJG31	10 3.2	3.2	2.6
*Bgl*II	pJG31	>10 8.5		>10
*Eco*RI	pJG31	>10 8.0		>10 4.8
*Kpn*I	pJG31	>10 8.3 2.0		>10 2.0

TABLE 6. Hybridization analysis of Δ*ilvD2076*

Chromosomal DNA digested with:	Plasmid *ilv* DNA probe	Fragment size (kb) of chromosomal DNA from the indicated *E. coli* strains that hybridized with the indicated probe	
		T31-4-4 (wild type)	CU655 (Δ*ilvD2076*)
*Pvu*I	pLC26-3 (*ilvGEDA*)	3.6	3.8
		2.5	2.5
		1.8	1.8
*Hin*dIII	pRD125 (*ilv'ED'*)	1.7	9.5
	pRD129 (*ilv'DA'*)	8.0	9.5
*Pst*I	pRD125 (*ilv'ED'*)	6.7	6.4
	pRD129 (*ilv'DA'*)	9.7	9.7
		6.7	6.4

restriction endonucleases and hybridized with pJG31 (Table 5). Comparison of the hybridization data indicated that this allele ends just distal to the *Bgl*II site at 18 kb in Fig. 2. Thus, the (*ilvGEDAYC-rep*)*2049* mutation deletes approximately 17 kb (from 1.0 to 18 kb in Fig. 2).

Analysis of the *ilvD2076* deletion. Hybridization of pLC26-3 (*ilvGEDA*) with a *Pvu*II digest of DNA from CU655 (Δ*ilvD2076*) identifies three *ilv*-specific *Pvu*II restriction fragments. The two *Pvu*II fragments from the proximal portion of the operon (1.8 and 2.5 kb) are of identical size to those from the wild type (Table 6). However, the largest *Pvu*II fragment in the digest of CU655 migrates slower than that from the wild type (Table 6). This indicates that there is an alteration of the structure of the DNA by this mutation between the *Pvu*II restriction sites at 6.2 and 6.4 kb in Fig. 2. Hybridization of the *ilv'ED'* and *ilv'DA'* probes to an *Hin*dIII digestion of DNA from CU655 identifies a single large *Hin*dIII fragment of 9.5 kb rather than the two discrete *Hin*dIII restriction fragments derived from wild-type DNA (Table 6). The single *Hin*dIII fragment of CU655 is 0.2 kb smaller than the sum of the two wild-type restriction fragments, and the data indicate that the *Hin*dIII restriction site at 6.4 kb is absent from the DNA of this strain. Digestion of DNA from CU655 with *Pst*I and subsequent hybridization with *ilv'ED'* and *ilv'DA'* probes indicate that the *Pst*I restriction site at approximately 6.7 kb (Fig. 2) is present in the DNA from CU655. Thus the *ilvD2076* mutation deletes approximately 200 bp from within *ilvD* between the *Pvu*II site at 6.2 kb and the *Pst*I site at 6.7 kb (Fig. 2).

DISCUSSION

This study determined the physical structure of several deletions of genes required for the biosynthesis of isoleucine and valine. Restriction endonuclease cleavage sites were used as fixed reference points for the determination of genetic structure. Genes were located relative to the restriction sites by the hybridization of homologous DNA species: chromosomal restriction endonuclease cleavage fragments and radioactively labeled plasmids containing cloned portions of the *ilvGEDA* operon. The physical dimensions of these deletions are indicated in Fig. 2. The largest mutation, Δ(*ilvGEDAYC-rep*)*2049*, deleted 17 kb of DNA, whereas the smallest, Δ*ilvD2076*, removed approximately 200 bp. Our analysis indicates that the *ilvGEDA* operon restriction site map previously determined by the analysis of bacteriophage (11) and plasmids (37) is identical to that in the genome.

***ilvA700*::Tn*5* derivatives; deletions *ilvGEDA724*::Tn*5*-131, *ilvGEDA723*::Tn*5*, and *ilvDA722*::Tn*5*.** Lines 1, 2, and 3 of Fig. 2 present the deletions derived by the curing of λ *b*221 *c*I857 *rex*::Tn*5*-131 from a lysogen of the *ilvA700*::Tn*5* parent, Δ*ilvGEDA724*::Tn*5*-131, Δ*ilvGEDA723*::Tn*5*, and Δ*ilvDA722*::Tn*5*. All originate from a single site in *ilvA*; 300 bp 3′ to the *Sal*I restriction site in *ilvA*, the point of Tn*5* insertion in *ilvA*. The Δ*ilvGEDA724*::Tn*5*-131 deletion extends from *ilvA* through the *ilv* genes to a point 200 to 300 bp distal to the *trpT* gene. The *Pvu*II and *Bgl*II restriction sites 2.9 kb proximal to the *ilvGEDA* operon are not included within the deletion. The reported nucleotide sequence of this region (42) indicates there are no *Pvu*II or *Bgl*II restriction sites within 130 bp of the *rrnC* operon terminator following *trpT*, which is consistent with the estimated extent of this deletion. The total size of the region removed from the genome in the Δ*ilvGEDA724*::Tn*5*-131 deletion is 8.3 kb. The *ilvGEDA723*::Tn*5* deletion extends from *ilvA* to within less than 80 bp 3′ of the *Pvu*II restriction site in *ilvG* (data not shown); a total distance of 4.2 kb. The smallest of the three deletions, *ilvDA722*::Tn*5*, extends from *ilvA* to a 400-bp region between the 5′ *Pvu*II and single *Hin*dIII restriction sites in *ilvD*, deleting approximately 1.6 kb.

The initial description of these mutants did not indicate the mechanism of their formation. Both the data presented here and our unpublished observations indicate that the transposons lie at the 3′ terminus of each of the deletions. This structural feature of these mutants is consistent with the deletion event having been transposon or IS*50* mediated, in a manner similar to that of bacteriophage Mu (10), IS*1* (25, 31), or IS*2* (30). To our knowledge, this is the first report of such Tn*5*-mediated deletions.

Although the details of their analysis were not in agreement with our final understanding (19), Berg et al. (3) proposed the correct mechanism for the effect of *ilvG* mutations on the expression of this operon. In part their analysis depended upon the conclusion that the truncated wild-type *ilvG* protein had AHAS activity. This conclusion was based upon comparison of the difference in AHAS activity in strains containing the Δ*ilvGEDA723*::Tn*5* and Δ*ilvGEDA724*::Tn*5*-131 mutations. Their analysis of these deletions indicated that the *ilv723* allele at least extended into *ilvE*. This allele had threefold-higher levels of AHAS activity than the other; combining this with other data, they concluded that the wild-type *ilvG* protein has AHAS activity. Our analysis of the physical dimensions of these mutations indicates that the proximal portion of *ilvG* (which would encode the truncated protein) remains intact in the Δ*ilvGEDA723*::Tn*5* mutant. However, our analysis of strains containing these deletions (Table 4) indicates the absence of an active AHAS polypeptide from the *ilvG* gene of wild-type *E. coli* K-12. This is consistent with the previously published analysis of the three AHAS isozymes that indicated that only AHAS I and AHAS III are active (reviewed in reference 8). Another observation that supports this conclusion is that plasmids that contain the wild-type *ilvG* gene (such as pRL5) do not complement strains such as PS1283 that lack functional *ilvB* and *ilvIH* (unpublished observations, J. Lopes).

The data in Table 4 and those presented by Berg et al. (3) contain two interesting observations. First, there is approximately a 30% increase in the total level of AHAS activity of strains that contain the *ilvGEDA723*::Tn*5* deletion relative to

strains that contain the intact wild-type *ilvG* gene. The second is the decrease in total AHAS activity in strains that contain either *ilvGEDA724*::Tn*5*-131 or (*ilvGEDAYC-rep*)*2049* mutations. The effects of these alleles on total AHAS activity may be due to the subunit structure of AHAS I (*ilvB*) and AHAS III (*ilvIH*). Genetic and biochemical evidence indicate that both isozymes contain large and small polypeptide subunits (8, 9, 36). Our analysis of the structure of *ilvG* demonstrated the formation of a 35,000-dalton polypeptide from the wild-type *ilvG* gene (19). It does not seem unreasonable to speculate that this truncated polypeptide interacts with the subunits of AHAS I and AHAS III in a manner that results in a net increase in total AHAS activity in cell extracts. The absence of an effect on AHAS activity by these alleles in strains lacking AHAS I and AHAS III is consistent with the observed changes being due to subunit interactions. The increase in total AHAS activity in strains that contain the *ilv723* allele may be the result of nucleic acid structure. The frameshift site that is present in the wild-type *ilvG* gene is polar (19, 21). This may decrease the stability of the *ilv* operon mRNA. The structure of the *ilvGEDA723*::Tn*5* mutation indicates that the terminus of the Tn*5* element is probably within 100 bp of the *Pvu*II site within *ilvG*. The structure that results from fusion of *ilvG* with the IS*50* element may result in a more stable *ilv* transcript, which would then yield an increased quantity of the 35,000-dalton protein. A clear understanding of these effects awaits an analysis of nucleic acid metabolism and structure of this allele.

***(ilvDAYC-rep)115* and *(ilvGEDAYC-rep)2049* deletions.** The (*ilvDAYC-rep*)*115* and (*ilvGEDAYC-rep*)*2049* deletions are considered together because they delete the *rep* gene. The (*ilvDAYC-rep*)*115* deletion was generated with UV light (17), whereas the (*ilvGEDAYC-rep*)*2049* deletion was selected on the basis of the loss of bacteriophage lambda from a secondary attachment site in *ilvC* (39). The extent of these deletions is presented on lines 4 and 5 of Fig. 2.

The Δ(*ilvDAYC-rep*)*115* mutation extends for 9.0 kb. The DNA removed by this deletion starts in close proximity to the *Hin*dIII restriction site in *ilvD* (Fig. 2), deleting the *Pst*I restriction site just 300 bp distal to that site. The terminus of the deletion most distal from the start of the *ilvGEDA* operon lies approximately 4.5 kb before *rho*. The Δ(*ilvGEDAYC-rep*)*2049* mutation encompasses the entire *ilv* gene cluster, removing 17.2 kb of the chromosome. This deletion extends to a 300-bp region between the *Hin*cII and *Hpa*I restriction sites 1.5 kb before the *ilvGEDA* operon. The other terminus lies within 2.0 kb of *rho*. The difference in the lengths of the (*ilvGEDAYC-rep*)*2049* and the *ilvGEDA724*::Tn*5*-131 deletions may prove useful in the analysis of the function of the 15K protein described by Gray et al. (12), since the region that encodes this polypeptide is bounded by these two deletions. The (*ilvGEDAYC-rep*)*2049* deletion was selected as a survivor of a lysogen of λy199 at the secondary lambda attachment in *ilvC* (41). Because of the method of isolation of this mutation, we had expected it to end in *ilvC*, which lies at the center of the deletion. Thus it would seem that this mutation was probably not generated by the imprecise excision of bacteriophage λ, since such deletions would be expected to be unidirectional from the site of insertion. This may indicate that the deletion event was not λ mediated or possibly that the original lysogen contained more than one copy of the bacteriophage.

Both the (*ilvGEDAYC-rep*)*2049* and (*ilvDAYC-rep*)*115* deletions extend into a region of the chromosome reported to contain the *rep* gene (38). Scott and Kornberg (32) have proposed that the *rep* protein is an ATPase that aids in the separation of DNA strands at the replication fork. Although *rep* mutants are not lethal, they are not able to support the replication of certain bacteriophage (5, 38). Infection occurs, but not proliferation, imparting a Gro⁻ phenotype to the cell (38). Strain M182 is sensitive to bacteriophage P2 (Table 7); however, upon transduction with either the (*ilvGEDAYC-rep*)*2049* (strain FD1042) or (*ilvDAYC-rep*)*115* (strain FD1040) deletions, the strain becomes resistant to lytic infection. Therefore, both deletions have inactivated the *rep* gene by removing all or part of it. Furthermore, neither contiguous plasmid pRD150 nor pJG31 can confer P2 sensitivity to strains containing either deletion. Since neither plasmid contains an active *rep* gene and the plasmids are contiguous on the chromosome, the *Hin*dIII restriction site at their boundary must be contained within the regulatory or coding regions of the gene. This *Hin*dIII restriction site is located 3.5 kb distal to *ilvC*. Tessman et al. (38) estimated the size of the *rep* gene to be 1.8 kb, based upon the size of its protein product. Therefore, the maximum extent of the *rep* gene is confined to a 3.6-kb region; 1.8 kb either side of the *Hin*dIII restriction site (at 14.5 kb in Fig. 2).

TABLE 7. Analysis of the Gro phenotype of strains containing the Δ(*ilvDAYC-rep*)*115* and Δ(*ilvGEDAYC-rep*)*2049* mutations

Strain	Genotype	Plasmid	Insert	Gro phenotype[a]
M182	Wild type			+
FD1040	Δ(*ilvDAYC-rep*)*115*			−
FD1040	Δ(*ilvDAYC-rep*)*115*	pRD150	*ilv'DAYC*	−
FD1040	Δ(*ilvDAYC-rep*)*115*	pJG31	*rho*	−
FD1042	Δ(*ilvGEDAYC-rep*)*2049*			−
FD1042	Δ(*ilvGEDAYC-rep*)*2049*	pRD150	*ilv'DAYC*	−
FD1042	Δ(*ilvGEDAYC-rep*)*2049*	pJG31	*rho*	−

[a] Sensitivity to bacteriophage P2.

***ilvD2076* deletion.** The extent of the *ilvD2076* deletion is presented in Fig. 2. The entire deletion is confined to a region between the first *Pvu*II restriction site in *ilvD* and the *Pst*I restriction site in *ilvD*. The size of the deletion is approximately 200 bp, based upon alterations in the electrophoretic mobilities of restriction fragments containing the deletion. This allele was formerly designated *ilvDA2076* because strains containing the deletion express neither *ilvD* nor *ilvA* (33). The polar effect of Δ*ilvD2076* on *ilvA* is similar to the phenomenon observed with strains containing the ochre mutation *ilvD188* (20), which do not express *ilvA*. The polarity of *ilvD* mutations on *ilvA* expression may reflect the site of transcriptional polarity located in *ilvD* or before *ilvA*, described initially by Smith et al. (34). This site may be of regulatory significance for the expression of *ilvA*, since mutations in *rho* (21, 34) and starvation for isoleucine (34) result in a disproportionate level of expression of threonine deaminase (product of *ilvA*) relative to the gene products of the proximal portions of the operon. Alternatively, the polar effect of mutations in *ilvD* on *ilvA* expression may be due to translational coupling of the genes for dihydroxy acid dehydratase and threonine deaminase, similar to that described for the *trp* operon (29).

In summary, our study of these deletions confirms the restriction site map that had been established by analysis of recombinant bacteriophage and plasmids. Using these techniques we believe one can detect overlaps between the hybridization probes and genomic restriction fragments as short as 50 to 100 bp. We were able to detect a deletion of approximately 200 bp. Both of these observations attest to

the sensitivity of this type of analysis. This technique may be useful in the future for the study of other deletion mutations or genetic rearrangements, since there is no necessity for the mobilization of the mutation for analysis. These results provide us with the tools for the analysis of the structure of the *ilvGEDA* genes in other enteric bacteria. These tools include the *(ilvGEDAYC-rep)2049* deletion, which lacks all homology to the operon probes. This gives us a null control for the hybridization of operon probes to the DNA of other *Enterobacteriaceae* under conditions of reduced stringency.

ACKNOWLEDGMENTS

We thank B. Ely, R. Musso, and E. A. Thompson for advice and criticism during the preparation of this manuscript and D. Chavis for typing it.

This work was supported in part by Public Health Service grant GM28021 from the National Institute of General Medical Sciences and Biomedical Support Grant 08-S7 RR07 160L06 from the National Institutes of Health.

LITERATURE CITED

1. **Bachmann, B. J.** 1983. Linkage map of *Escherichia coli* K-12, edition 7. Microbiol. Rev. **47**:180–230.
2. **Beck, E., G. Ludwig, E. A. Auerswald, B. Reiss, and H. Schaller.** 1982. Nucleotide sequence and exact location of the neomycin phosphotransferase gene from transposon Tn5. Gene **19**:327–336.
3. **Berg, C. M., K. J. Shaw, and D. E. Berg.** 1980. The *ilvG* gene is expressed in *Escherichia coli* K-12. Gene **12**:165–170.
4. **Boros, I., A. Kiss, and P. Venetianer.** 1979. Physical map of the seven ribosomal genes of *Escherichia coli*. Nucleic Acids Res. **6**:1817–1830.
5. **Calendar, R., B. Lindquist, G. Sironi, and A. J. Clark.** 1970. Characterization of Rep$^+$ mutants and their interaction with P2 phage. Virology **40**:72–83.
6. **Davis, R. W., D. Botstein, and J. R. Roth.** 1980. Advanced bacterial genetics. Cold Spring Harbor Laboratory, Cold Spring Harbor, N.Y.
7. **Davis, R. W., M. Thomas, J. Cammeron, T. St. P. John, S. Scherer, and R. A. Padgett.** 1980. Rapid DNA isolation for enzymatic and hybridization analysis. Methods Enzymol. **65**:404–414.
8. **De Felice, M., M. Levinthal, M. Iaccarino, and J. Guardiola.** 1979. Growth inhibition as consequence of antagonism between related amino acids: effect of valine in *Escherichia coli* K-12. Microbiol. Rev. **43**:22–58.
9. **Eoyang, L., and P. M. Silverman.** 1984. Purification and subunit composition of acetohydroxy acid synthase I from *Escherichia coli* K-12. J. Bacteriol. **157**:184–189.
10. **Faelen, M., and A. Toussaint.** 1978. Mu-mediated deletions in the chromosome of *Escherichia coli* K-12. J. Bacteriol. **136**:477–483.
11. **Gray, J. E., D. W. Patin, and D. H. Calhoun.** 1981. Identification of the protein products of the *rrnC*, *ilv*, *rho* region of the *Escherichia coli* K-12 chromosome. Mol. Gen. Genet. **183**: 428–436.
12. **Gray, J. E., J. W. Wallen, and D. H. Calhoun.** 1982. Identification of a protein of 15,000 daltons related to isoleucine-valine biosynthesis in *Escherichia coli* K-12. J. Bacteriol. **151**:127–134.
13. **Hirsh, D.** 1970. Tryptophan tRNA of *Escherichia coli*. Nature (London) **228**:57.
14. **Hoopes, B. C., and W. R. McClure.** 1981. Studies on the selectivity of DNA precipitation by spermine. Nucleic Acids Res. **9**:5493–5504.
15. **Jorgensen, P., J. Collins, N. Fiil, and K. von Meyenburg.** 1978. A ribosomal RNA gene, *rrnC*, of *Escherichia coli*, mapped by specialized transducing *lambdailv* and *lambdarbs* phages. Mol. Gen. Genet. **163**:223–228.
16. **Jorgensen, R. A., S. J. Rothstein, and W. S. Reznikoff.** 1979. A restriction enzyme cleavage map of Tn5 and location of a region encoding neomycin resistance. Mol. Gen. Genet. **117**:65–72.
17. **Kiritani, K., T. Matsuno, and Y. Ikeda.** 1965. Genetic and biochemical studies on isoleucine and valine requiring mutants of *Escherichia coli*. Genetics **51**:341–349.
18. **Kline, E. L., S. Brown, G. Coleman, Jr., and H. E. Umbarger.** 1974. Regulation of isoleucine-valine biosynthesis in an *ilvDAC* deletion strain of *Escherichia coli* K-12. Biochem. Biophys. Res. Commun. **57**:1144–1151.
19. **Lawther, R. P., D. H. Calhoun, C. W. Adams, C. A. Hauser, J. Gray, and G. W. Hatfield.** 1981. Molecular basis of valine resistance in *Escherichia coli* K-12. Proc. Natl. Acad. Sci. U.S.A. **78**:922–925.
20. **Lawther, R. P., and G. W. Hatfield.** 1977. Biochemical characterization of an *Escherichia coli hisT* strain. J. Bacteriol. **130**: 552–557.
21. **Lawther, R. P., and G. W. Hatfield.** 1978. A site for tRNA mediated regulation of the *ilvOEDA* operon of *Escherichia coli* K-12. Mol. Gen. Genet. **167**:227–234.
22. **Maniatis, T., E. F. Fritsch, and J. Sambrook.** 1982. Molecular cloning. Cold Spring Harbor Laboratory, Cold Spring Harbor, N.Y.
23. **Marsh, N. J., and D. E. Duggan.** 1972. Ordering of mutant sites in the isoleucine-valine genes of *Escherichia coli* by use of merogenotes derived from F14: a new procedure for fine-structure mapping. J. Bacteriol. **109**:730–740.
24. **Maxam, A. M., and W. Gilbert.** 1980. Sequencing end-labeled DNA with base-specific chemical cleavage. Methods Enzymol. **65**:499–560.
25. **Mickel, S., E. Ohtsubo, and W. Bauer.** 1977. Heteroduplex mapping of small plasmids derived from R-factor R12: *in vivo* recombination occurs at IS1 insertion sequences. Gene **2**:193–210.
26. **Miller, J. H.** 1972. Experiments in molecular genetics. Cold Spring Harbor Laboratory, Cold Spring Harbor, N.Y.
27. **Morgan, E. A., and M. Nomura.** 1979. Deletion analysis of the expression of rRNA genes and associated tRNA genes carried by a λ transducing bacteriophage. J. Bacteriol. **137**:507–516.
28. **Newman, T. C., and M. Levinthal.** 1980. A new map location for the *ilvB* locus of *Escherichia coli*. Genetics **96**:59–97.
29. **Oppenheim, D. S., and C. Yanofsky.** 1980. Translational coupling during the expression of the tryptophan operon of *Escherichia coli*. Genetics **95**:785–795.
30. **Peterson, P. A., D. Ghosal, H. Sommer, and H. Saedler.** 1979. Development of a system useful for studying the formation of unstable alleles of IS2. Mol. Gen. Genet. **173**:15–21.
31. **Reif, H. J., and H. Saedler.** 1975. Chromosomal rearrangements in the *gal* region of *E. coli* K-12 after integration of IS1, p. 81–91. *In* A. I. Burkhari, J. A. Shapiro, and S. L. Adhya (ed.), DNA insertion elements, plasmids and episomes. Cold Spring Harbor Laboratory, Cold Spring Harbor, N.Y.
32. **Scott, J. F., and A. Kornberg.** 1978. Purification of the *rep* protein of *Escherichia coli*: the ATPase which separates duplex DNA strands in advance of replication. J. Biol. Chem. **253**: 3292–3297.
33. **Smith, J. M., F. J. Smith, and H. E. Umbarger.** 1979. Mutations affecting the formation of acetohydroxy acid synthase II in *Escherichia coli* K-12. Mol. Gen. Genet. **169**:299–314.
34. **Smith, J. M., D. E. Smolin, and H. E. Umbarger.** 1976. Polarity and the regulation of the *ilv* gene cluster in *Escherichia coli* K-12. Mol. Gen. Genet. **148**:111–124.
35. **Southern, E.** 1975. Detection of specific sequences among DNA fragments separated by gel electrophoresis. J. Mol. Biol. **98**: 503–517.
36. **Squires, C., M. DeFelice, J. Devereux, and J. M. Calvo.** 1983. Molecular structure of *ilvIH* and its evolutionary relationship to ilvG in *Escherichia coli* K-12. Nucleic Acids Res. **11**:5299–5313.
37. **Subrahmanyam, C. S., G. M. McCorkle, and H. E. Umbarger.** 1980. Physical location of the *ilvO* determinant in *Escherichia coli* K-12 deoxyribonucleic acid. J. Bacteriol. **142**:547–555.
38. **Tessman, I., J. S. Fassler, and D. C. Bennett.** 1982. Relative map location of the *rep* and *rho* genes of *Escherichia coli*. J.

Bacteriol. **151**:1637–1640.
39. **Watson, M. D., J. Wild, and H. E. Umbarger.** 1979. Positive control of *ilvC* expression in *Escherichia coli* K-12: identification and mapping of regulatory gene *ilvY*. J. Bacteriol. **139**: 1014–1020.
40. **Wild, J., J. M. Smith, and H. E. Umbarger.** 1977. *In vitro* synthesis of beta-galactosidase with *ilv-lac* fusion deoxyribonucleic acid template. J. Bacteriol. **132**:876–883.
41. **Williams, A. L., N. Baylor, and M. Ensor.** 1981. Evidence for the site of lambda insertion in the *ilv* gene cluster of *Escherichia coli* K-12. J. Bacteriol. **147**:691–693.
42. **Young, R. A.** 1979. Transcription termination in the *Escherichia coli* ribosomal RNA operon *rrnC*. J. Biol. Chem. **254**: 12725–12731.